THE JOURNAL OF BIOLOGICAL CHEMISTRY VOL. 281, NO. 1, pp. 365–373, January 6, 2006

A Role for Kif17 in Transport of Kv4.2*[S]

Received for publication, August 12, 2005, and in revised form, October 14, 2005 Published, JBC Papers in Press, October 28, 2005, DOI 10.1074/jbc.M508897200

Po-Ju Chu[1], **Jacqueline F. Rivera**[1], **and Don B. Arnold**[2]

From the Department of Biology and Program in Molecular and Computational Biology, University of Southern California, Los Angeles, California 90089

Although kinesins are known to transport neuronal proteins, it is not known what role they play in the targeting of their cargos to specific subcellular compartments in neurons. Here we present evidence that the K^+ channel Kv4.2, which is a major regulator of dendritic excitability, is transported to dendrites by the kinesin isoform Kif17. We show that a dominant negative construct against Kif17 dramatically inhibits localization to dendrites of both introduced and endogenous Kv4.2, but those against other kinesins found in dendrites do not. Kv4.2 colocalizes with Kif17 but not with other kinesin isoforms in dendrites of cortical neurons. Native Kv4.2 and Kif17 coimmunoprecipitate from brain lysate, and introduced, tagged versions of the two proteins coimmunoprecipitate from COS cell lysate, indicating that the two proteins interact, either directly or indirectly. The interaction between Kif17 and Kv4.2 appears to occur through the extreme C terminus of Kv4.2 and not through the dileucine motif. Thus, the dileucine motif does not determine the localization of Kv4.2 by causing the channel to interact with a specific motor protein. In support of this conclusion, we found that the dileucine motif mediates dendritic targeting of CD8 independent of Kif17. Together our data show that Kif17 is probably the motor that transports Kv4.2 to dendrites but suggest that this motor does not, by itself, specify dendritic localization of the channel.

The electrophysiological properties of neurons arise from an intricate spatial distribution of ion channels and receptors on the plasma membranes of these cells. The complexity of this distribution is illustrated by experiments showing that nearly 500 distinct proteins reside at the postsynaptic density (1), each of which must be regulated at over 10,000 postsynaptic sites in a typical cortical pyramidal neuron (2). The fidelity of this distribution is critical, since mislocalization of ion channels and receptors can lead to the breakdown of signal transduction cascades that are essential for physiological functioning of neurons (3). These and many other observations suggest that neurons can create and maintain complex subcellular distributions of proteins. However, little is known about how this is accomplished at the molecular level.

Progress toward elucidating the molecular mechanisms underlying subcellular localization of neuronal proteins has been made by identifying targeting motifs within the primary structure of transmembrane proteins that are localized in distinct subcellular compartments (4–9). The voltage-gated K^+ channel Kv4.2 has served as a model for dendritic targeting (10). It is a major regulator of excitability in the dendrites of hippocampal pyramidal cells in the CA1 region, and its presence in dendrites but not axons is thought to account for the propagation of action potentials exclusively in the latter compartment (11). We previously identified a 16-amino acid dileucine-containing motif, located in the C terminus of Kv4.2 (10), that is both necessary for dendritic targeting of the channel and sufficient to induce nonspecifically localized transmembrane proteins to target to dendrites.

Recent experiments suggest that some transmembrane proteins are localized in dendrites as a result of directed vesicular transport (12) and that transport of proteins from the cell body to dendrites is mediated by kinesins (13, 14). In light of these findings, we sought to identify the kinesin isoform responsible for transporting Kv4.2 and to examine a possible role for this kinesin in dendritic targeting of the channel. By screening a series of dominant negative constructs directed against specific kinesins, we identified Kif17 as being necessary for localization of Kv4.2. We established that Kif17 and Kv4.2 probably interact by showing that native forms of the two proteins colocalize in dissociated neurons and coimmunoprecipitate from brain lysate. Introduced forms of the two proteins coimmunoprecipitate when coexpressed in COS cells. The interaction between Kv4.2 and Kif17, which may be direct or indirect, is mediated by the extreme C terminus of the channel and not by the dileucine motif. Together, our results indicate that Kv4.2 is probably transported to the dendrites by Kif17.

EXPERIMENTAL PROCEDURES

DNA Constructions—Kif17 was amplified from mouse cDNA using PCR. The dominant negative kinesin constructs were generated by replacing the motor domains of the respective kinesin molecules with GFP[3] or YFP and placing the resulting constructs in the mammalian expression vector GW. For DNKif21B, amino acids 2–530 were deleted; for DNKif5B, amino acids 2–366 were deleted; for DNKif5A, amino acids 2–373 were deleted; and for DNKif17, amino acids 2–323 were deleted. Because KifC2 has its motor region on the C terminus, amino acids 370–792 were deleted and replaced with YFP. Two tagged constructs were made for wild-type kinesins, one with GFP or YFP and the other with a double HA epitope tag. All of the tags were on the N terminus except those for KifC2, which was tagged on the C terminus. Kv4.2 was tagged with GFP on the N terminus to give GFP-Kv4.2. GFP-Kv4.2ΔC was made from GFP-Kv4.2 by deleting 30 amino acids at the extreme C terminus. GFP-Kv4.2C consists of the last 30 amino acids (positions 601–630) of Kv4.2 tagged at the N terminus with GFP. GFP-Kv4.2ΔLL consists of a GFP-tagged version of Kv4.2 with amino acids 474–489 deleted. GFP-Kv4.2TΔLLΔC consists of a GFP-tagged version of the cytoplasmic tail of Kv4.2 with amino acids 474–489 and 601–630 deleted. YFP-LL was made by tagging the amino acids 474–489 of Kv4.2 with YFP at the N terminus. The construct Kv4.2ΔN was made by delet-

* This work was supported by NINDS, National Institutes of Health, Grant RO1 NS-41963 and a grant from the Whitehall Foundation (both to D. B. A.). The costs of publication of this article were defrayed in part by the payment of page charges. This article must therefore be hereby marked "*advertisement*" in accordance with 18 U.S.C. Section 1734 solely to indicate this fact.

[S] The on-line version of this article (available at http://www.jbc.org) contains Figs. S1–S4.

[1] These two authors contributed equally to this work.

[2] To whom correspondence should be addressed: Dept. of Biology, University of Southern California, 1050 Childs Way, MCB 204b, Los Angeles, CA 90089-2910. Tel.: 213-821-1266; Fax: 213-821-1818; E-mail: darnold@usc.edu.

[3] The abbreviations used are: GFP, green fluorescent protein; YFP, yellow fluorescent protein; HA, hemagglutinin; PBS, phosphate-buffered saline; DNKif, dominant negative kinesin; ADR, axon/dendrite ratio; ER, endoplasmic reticulum.

ing amino acids 2–31 of Kv4.2. The inducible Kv4.2, CD8, and CD8-LL constructs were generated by inserting Kv4.2-MYC, CD8, and CD8-LL (10) into the pIND vector (Invitrogen). Other plasmids used were the β-galactosidase expression plasmid pCMVβ (Stratagene) and pVgRXR (Invitrogen).

Preparation of Dissociated Cell Cultures—Briefly, cortices from either embryonic day 18 Sprague-Dawley rats or embryonic day 18 CD1 mice were dissected in Hanks' balanced salt solution (Invitrogen). Cortices were dissociated by incubating in papain enzyme solution (100 mM $CaCl_2$, 50 mM EDTA, 0.1% β-mercaptoethanol (ICN), 100 units of papain (Sigma)) in Earle's balanced salt solution (final pH 7.4) for 30 min. Dissociated cortical neurons were plated on polylysine-coated glass coverslips at a density of 1×10^5 neurons/well in neurobasal medium (Invitrogen) supplemented with 10 ml/liter GlutaMAX (Invitrogen), 1 μg/ml gentamicin (Invitrogen), 20 ml/liter B-27 supplement (Invitrogen), and 50 ml/liter fetal bovine serum (Invitrogen). The medium was changed after 1 h to neurobasal medium without serum and changed every 4 days thereafter. Dissociated cell cultures at 11–15 days *in vitro*, and COS-7 cells were transfected with DNA constructs using either the Calphos transfection system (BD Biosciences) or Effectene transfection reagent (Qiagen), respectively, using procedures suggested by the respective manufacturers.

Immunocytochemisty of Dissociated Neuronal Cultures—The cells were fixed with 4% paraformaldehyde for 5 min and washed with phosphate-buffered saline (PBS). This was followed by a permeabilization step and a blocking step with blocking solution (1% bovine serum albumin, 5% normal goat serum, 0.1% Triton X-100 in PBS). After blocking, primary antibody was diluted in blocking solution and added for 30–120 min. Secondary antibody was diluted in blocking solution and added for 30 min in the dark. Primary antibody dilutions were as follows: rabbit anti-GFP 1:2000 (BD Biosciences), mouse anti-MYC 1:1000 (Covance), mouse anti-HA 1:1000 (Covance), rabbit anti-Kv4.2 1:2000 (Alomone Labs), rabbit anti-GluR2 1:200 (Chemicon), and rabbit anti-Kif17 (Abcam). Antibody labeling was then visualized by incubating cells with Alexa 488-, Alexa 594-, and Alexa 647-conjugated secondary antibodies (Molecular Probes, Inc., Eugene, OR).

Slice Immunocytochemistry—Culturing of slices was previously described (15). Following incubation for 4 h, the slices were transfected using the Helios gene gun (Bio-Rad). Slices were then stained for total protein after incubation for 3 days. Slices were fixed with 2.5% paraformaldehyde and 4% sucrose for 30 min, incubated in blocking solution (2% bovine serum albumin, 10% normal goat serum, 0.25% Triton X-100 in PBS) for 1 h followed by incubation with primary antibody for 1 h. Primary antibodies used were as follows: rabbit anti-GFP, 1:2000 (BD Biosciences); chicken anti-β-galactosidase 1:1000 (ICL), mouse anti-MYC 1:500 (Covance), and mouse anti-CD8 1:50 (Dako). They were then incubated in secondary antibody for 1 h. Antibody labeling was visualized by Alexa 594-, Alexa 488-, and Alexa 647-conjugated secondary antibodies (Molecular Probes). Slices were then cleared with xylene and mounted.

Induction of Expression —Constructs driven by the pIND promoter (Invitrogen) were cotransfected into neurons in cortical slices with the pVgRXR vector and incubated for 24 h. They were subsequently induced using ponasterone A (Invitrogen), which was added to a final concentration of 5 μM in the slice culture medium. Immunocytochemistry was performed after an additional 48 h of incubation.

Co-immunoprecipitation and Western Blotting—COS cells were cultured in 60-mm dishes to about 80% confluent and transfected with Effectene transfection reagent (Qiagen) using 0.5 μg of each expression plasmid according to the manufacturer's protocol. Cells were then washed twice with PBS 48 h after transfection and lysed in ice-cold lysis buffer (10 mM Tris-HCl, pH 8.0, 150 mM NaCl, 1 mM EDTA, and 1% (v/v) Nonidet P-40) with protease inhibitors (0.12 mg/ml phenylmethylsulfonyl fluoride, 2 μg/ml leupeptin, 1 μg/ml aprotinin, and 1 μg/ml pepstatin A). The following steps were carried out at 4 °C unless otherwise noted. After cell lysates were incubated for 1 h, insoluble material was removed by centrifugation at 16,000 × *g* for 15 min, and the supernatants normalized for protein content were precleared with protein A-agarose (ImmunoPure immobilized protein A; Pierce) for 1 h. Rabbit anti-GFP antibody or normal rabbit IgG (BD Biosciences) was added to precleared supernatants and incubated with inversion overnight. Protein A-agarose was added to the immune complexes, and the mixtures were further incubated with inversion for 3 h followed by centrifugation at 9,000 × *g* for 5 min. The precipitates were washed three times with 10 mM Tris-HCl, pH 8.0, 150 mM NaCl, 1 mM EDTA, and 0.1% (v/v) Nonidet P-40 and eluted in SDS sample buffer (125 mM Tris-HCl, pH 6.8, 80 mM EDTA, 4% SDS, 30% (v/v) glycerol, and 0.1 mg/ml bromphenol blue). For immunoprecipitation of endogenous Kv4.2 from brain lysate, the preparation of postnuclear supernatant and the immunoprecipitation reaction were performed as previously described (16) with modification. Briefly, adult mouse brains were homogenized in ice-cold homogenization buffer (8% sucrose, 20 mM β-glycerophosphate, 3 mM imidazole, pH 7.4) with protease inhibitors. The brain postnuclear supernatant was collected by removing pellets under centrifugation of 1,000 × *g* for 10 min. The postnuclear supernatant was further diluted in lysis buffer (150 mM NaCl, 1 mM EDTA, 1 mM EGTA, 1% Triton X-100, 2.5 mM sodium pyrophosphate, 1 mM β-glycerophosphate, 1 mM Na_3VO_4, and 20 mM Tris-HCl, pH 7.5, with protease inhibitors) and incubated at 4 °C for 1 h. Extracts were then clarified twice by centrifugation at 15,000 × *g* for 5 min to remove insoluble material. Following preclearing with protein A-agarose for 1 h, the resulting brain lysate was incubated with rabbit anti-Kv4.2 polyclonal antibody (Alomone Labs) or normal rabbit IgG with inversion for overnight. Protein A-agarose was added to the immunocomplexes, and the mixtures were further incubated with inversion for 3 h followed by centrifugation at 9,000 × *g* for 5 min. The precipitates were washed five times with PBS and eluted in SDS sample buffer.

For Western blotting, protein samples were resolved by SDS-PAGE and transferred to nitrocellulose membranes (Bio-Rad). The resulting blots were blocked for 1 h in Tris-buffered saline with Tween 20 (TBST; 500 mM Tris-HCl, pH 7.5, 150 mM NaCl, and 0.05% (v/v) Tween 20) containing 5% nonfat dry milk. The blots were incubated with specific primary antibodies mouse anti-HA (1:1,000; Covance), mouse anti-GFP (1:500; Molecular Probes), rabbit anti-Kif17 (1:1000; Abcam), or rabbit anti-Kv4.2 (1:2,000; Alomone Labs) at 4 °C overnight and washed three times in TBST, followed by incubation with corresponding horseradish peroxidase-conjugated secondary antibodies goat anti-mouse (1:10,000; Jackson ImmunoResearch) or donkey anti-rabbit (1:5,000; Amersham Biosciences) at room temperature. After washing three times in TBST, the blots were visualized using Western Lightning Chemiluminescence Regent (PerkinElmer Life Sciences) followed by exposure to BioMax Light films (Eastman Kodak Co.).

Image Capture and Analysis—All imaging was done on a Bio-Rad MRC-1024 confocal microscope. Each cell was imaged as a stack of optical sections, 1 μm in depth apart. All calculations were performed on compressed images. For each cell, images of expressed constructs were taken using the 488-, 568-, and 647-nm laser lines at the same settings. Each construct was imaged in cells that were taken from at least three different slices.

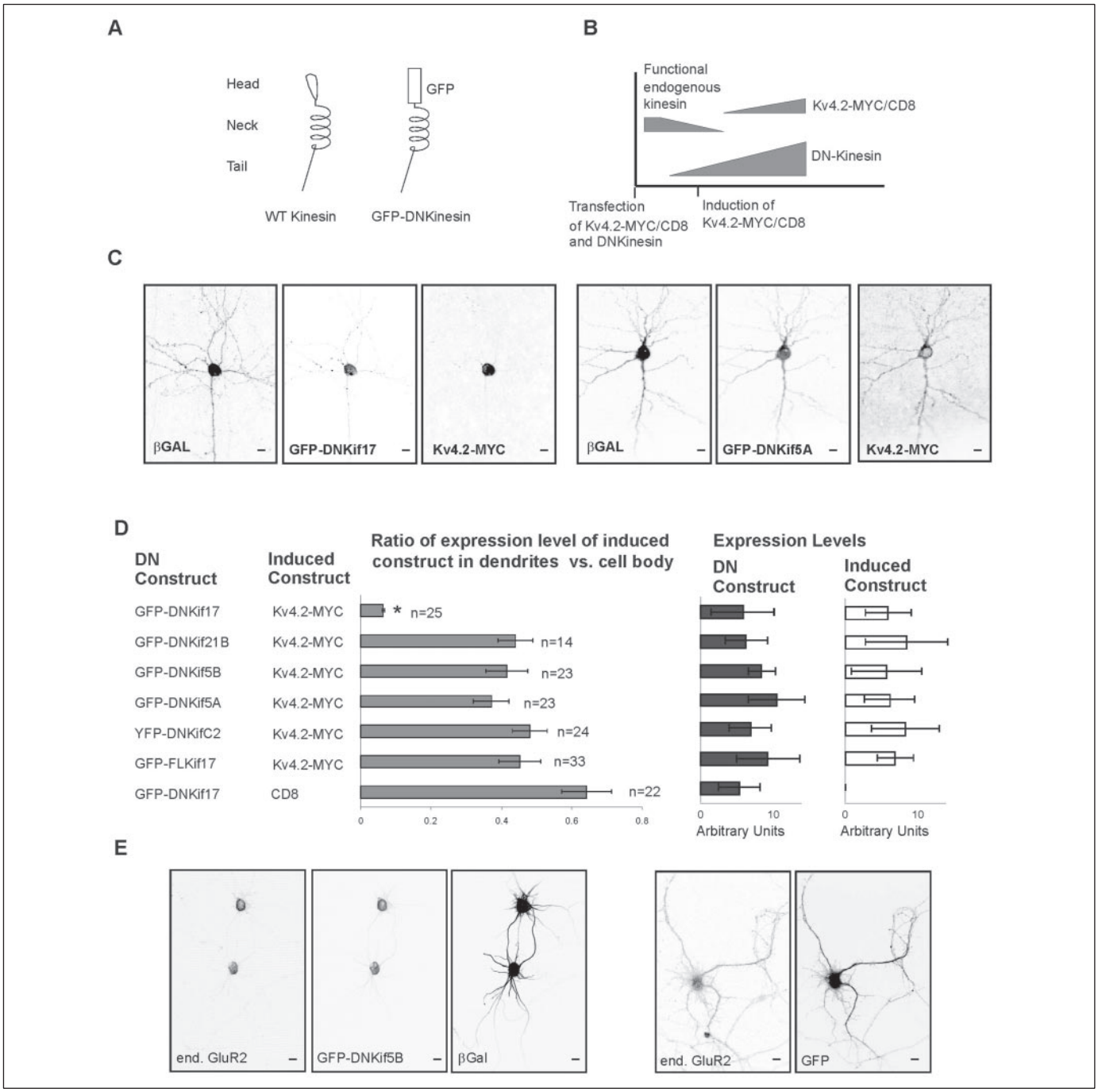

FIGURE 1. **A dominant negative variant of Kif17 blocks localization of introduced Kv4.2.** *A*, dominant negative variants of different kinesin isoforms (GFP-DNKinesin) were made by replacing the motor domains of wild-type kinesins (*WT Kinesin*) with GFP. *B*, schematic of the time course of experiments using dominant negative kinesins. One of five dominant negative kinesin constructs was initially expressed in neurons in cortical slices for 24 h, allowing time to dimerize with endogenous kinesins in these cells. Subsequently, either MYC-tagged Kv4.2 or CD8 was induced for 48 h in the same cells. β-Galactosidase (*βGAL*) was also expressed in the same cells as a counterstain. Slices were then fixed and stained for either MYC or CD8 to determine whether localization of the induced protein had been blocked. *C*, cells expressing Kv4.2 and either GFP-DNKif17 or GFP-DNKif5A (and β-galactosidase as a counterstain). GFP-DNKif17 blocked localization to dendrites of Kv4.2, whereas GFP-DNKif5A did not. *D*, expression of GFP-DNKif17 prior to expression of Kv4.2-MYC caused the channel to concentrate in the cell body, with a dendrite/cell body ratio of 0.06 ± 0.003 ($n = 25$). In contrast, in cells expressing GFP-DNKif21B, GFP-DNKif5B, GFP-DNKif5A, or YFP-DNKifC2, Kv4.2-MYC expressed with dendrite/cell body ratios of 0.44 ± 0.05 ($n = 14$), 0.42 ± 0.06 ($n = 23$), 0.37 ± 0.05 ($n = 23$), and 0.48 ± 0.05 ($n = 24$), respectively. GFP-FLKif17 refers to tagged, full-length Kif17, which did not block dendritic localization of Kv4.2-MYC (dendrite/cell body ratio = 0.45 ± 0.06, $n = 33$). GFP-DNKif17 failed to block dendritic transport of CD8 (dendrite/cell body ratio = 0.64 ± 0.07, $n = 22$), indicating that it did not block protein transport nonspecifically. The *asterisk* indicates that the average dendrite/cell body ratio for Kv4.2-MYC in cells expressing GFP-DNKif17 was significantly different from all similarly calculated ratios for the channel in cells expressing dominant negative kinesin variants other than GFP-DNKif17 shown in this figure ($p < 0.0001$). Average expression levels of Kv4.2 and of the dominant negative (*DN*) constructs did not vary dramatically for different dominant negative constructs. Note that expression levels are measured in arbitrary units of fluorescence that are the same for each measurement. *E*, GFP-DNKif5B blocked localization of endogenous GluR2 in a cortical neuron in dissociated culture. When only GFP is expressed in a similar cell, endogenous GluR2 is found throughout the dendrites. *Scale bars*, 10 μm.

For neurons in a slice, the axon was identified as a single process that (i) projected in a direction opposite to that of the cortical surface and the apical dendrite and (ii) was clearly longer than any dendrite (15). To quantify the degree of polarization in the distribution of a particular protein, we calculated the axon/dendrite ratio (ADR). ADR was defined as the ratio of the amount of protein in the axon *versus* that in the

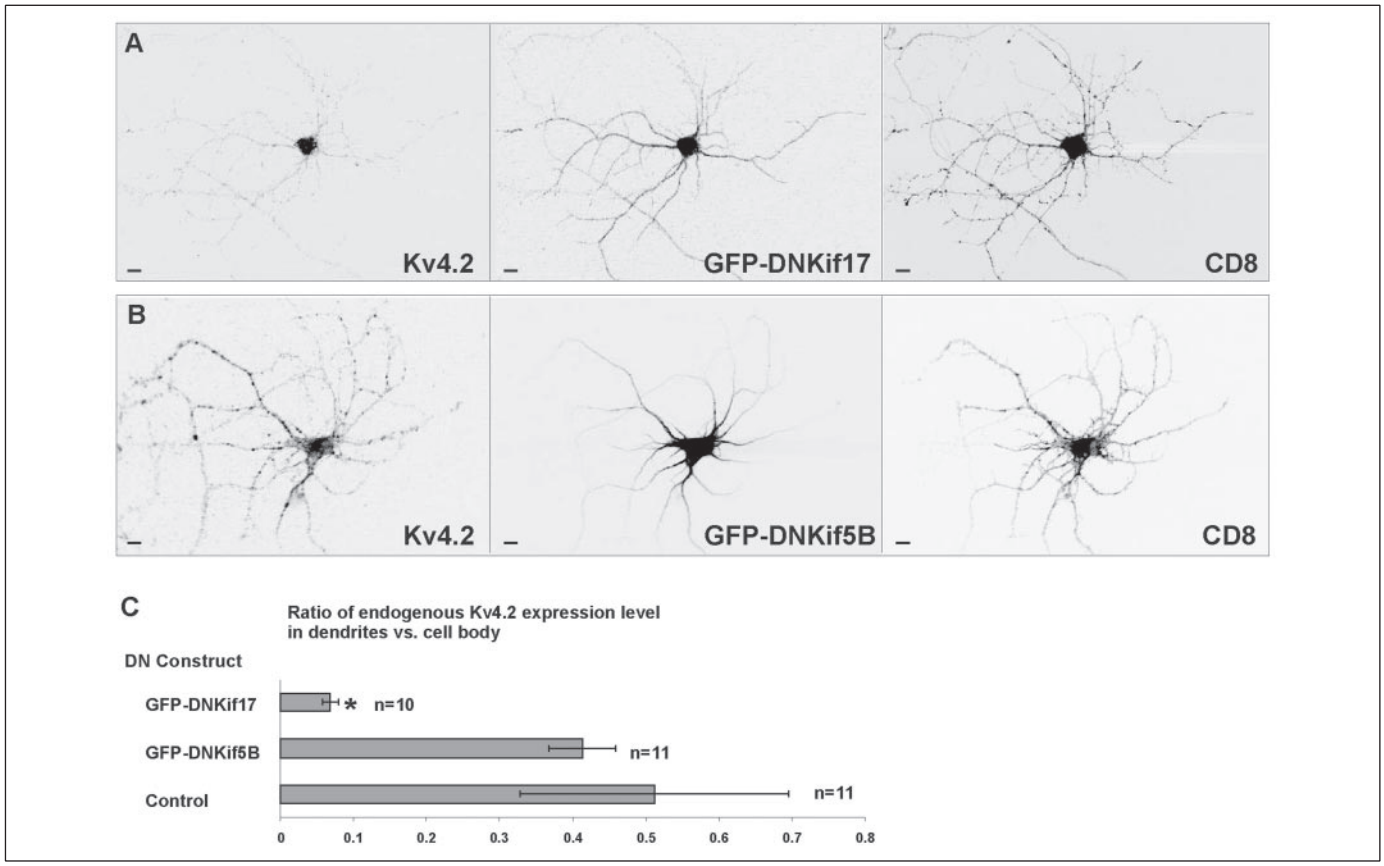

FIGURE 2. **A dominant negative (*DN*) variant of Kif17 blocks localization of endogenous Kv4.2.** *A*, a rat cortical neuron from a dissociated culture is pictured 48 h after expression of GFP-DNKif17. Staining for endogenous Kv4.2 shows a high density of the channel in the cell body and a low density in dendrites, consistent with Kif17 being necessary for localization of Kv4.2 to dendrites. In contrast, CD8 is localized throughout the entire cell, indicating that protein transport was not inhibited nonspecifically. *B*, endogenous Kv4.2 is localized throughout the dendrites following expression of GFP-DNKif5B. CD8 is localized throughout the cell. *C*, the dendrite to cell body ratio for endogenous Kv4.2 is 0.06 ± 0.01 for cells expressing GFP-DNKif17, 0.4 ± 0.05 for cells expressing GFP-DNKif5B, and 0.5 ± 0.2 for untransfected cells (control). The *asterisk* indicates that there is a significant difference ($p < 0.0001$) between the ratio for cells expressing GFP-DNKif17 and the ratios for either cells expressing GFP-DNKif5B or untransfected cells. *Scale bars*, 10 μm.

dendrites normalized by the ratio of the volume of the axon *versus* that of the dendrite (10). This normalization was used because the axonal compartments tended to be much smaller than the dendritic compartments and could vary greatly in size. Expression levels were determined by calculating the total amount of fluorescence associated with a given protein in the entire cell. Only expression levels of proteins detected by the same antibodies were compared. The ratio of the expression level of Kv4.2 in the dendrites *versus* the cell body was calculated as follows. The average intensity of fluorescence associated with Kv4.2 staining was measured in the cell body and at points 25 μm from the cell body on three dendrites for cells in dissociated culture and on the apical dendrite alone for cells in slices. The ratio of the dendritic value to that of the cell body was calculated for individual neurons. All analyses were performed by blinded observers.

RESULTS

Identification of a Kinesin Isoform Necessary for Localization of Kv4.2—In order to understand the contribution of kinesin motors to dendritic targeting of Kv4.2, we sought to identify the kinesin isoform responsible for transporting this channel. We created dominant negative variants of five different kinesin family members, Kif5A, Kif5B, Kif17, Kif21B, and KifC2, by replacing their motor domains with GFP (Fig. 1*A*). We chose Kif17 and Kif5B, because they have already been shown to transport the dendritic ion channels, NR2B and GluR2, respectively (13, 14, 17). Moreover, dominant negative variants of Kif17 and Kif5B were shown to block transport of the two channels (14, 17). Kif5A, Kif21B, and KifC2 were chosen, because they are found in dendrites (18–20). We assayed the effectiveness of dominant negative kinesins (DNKifs) by assessing whether any of them blocked dendritic localization of introduced Kv4.2 in neurons in cortical slices. The effects of DNKifs could be assessed accurately only if they were expressed at levels sufficient to block endogenous kinesin prior to expression of Kv4.2-MYC. To accomplish this, DNKifs under the control of a constitutively active cytomegalovirus promoter were expressed in cortical neurons, and 24 h subsequently, Kv4.2-MYC was expressed in the same cells using an inducible ecdysone promoter (Fig. 1*B*).

Examination of the expression patterns of Kv4.2 in cells in which DNKifs had been expressed revealed a striking pattern; in cells where a dominant negative variant of the Kif17 molecule (GFP-DNKif17) was expressed, Kv4.2-MYC was almost completely confined to the cell body, whereas in cells where GFP-DNKif5A, GFP-DNKif5B, YFP-DNKifC2, or GFP-DNKif21B was expressed, Kv4.2-MYC was present throughout the dendrites at distances over 150 μm from the cell body (Fig. 1*C*, data not shown). In order to quantify the effect of particular DNKifs on localization of Kv4.2, we calculated the ratio of the expression level of the tagged channel in the dendrites *versus* that in the cell body. Lower ratios indicate that a protein is localized preferentially to the cell body, consistent with blocking of transport to the dendrites of that protein. The quantified results corroborated our qualitative observations. In cells expressing GFP-DNKif17, the dendrite/cell body ratio of Kv4.2-MYC was 0.06 ± 0.003 ($n = 25$; Fig. 1*D*), indicating that the channel was

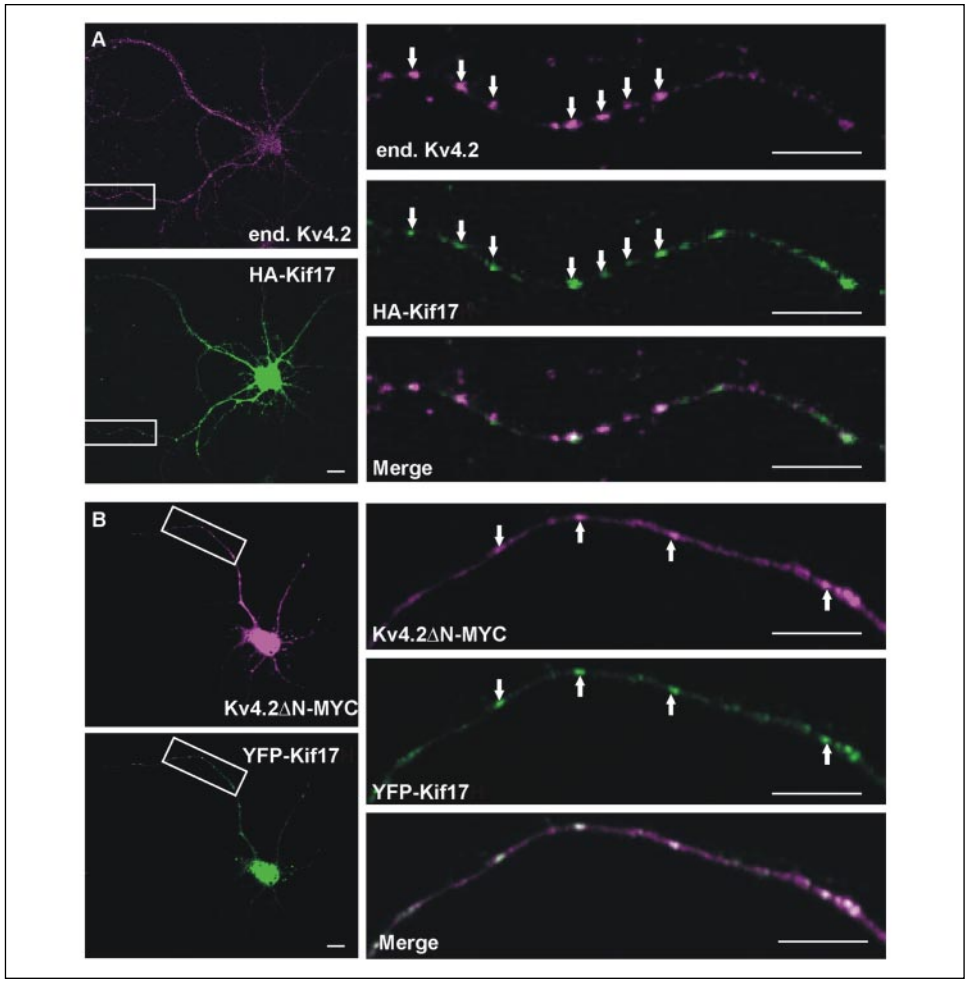

FIGURE 3. **Kv4.2 colocalizes with Kif17.** *A*, a rat cortical neuron in dissociated culture transfected with HA-Kif17 and stained for endogenous Kv4.2 (*purple*) and for HA (*green*). The two proteins show a high degree of colocalization (*white*). *B*, a rat cortical neuron expressing Kv4.2ΔN-MYC (*purple*) and YFP-Kif17 (*green*). Note that Kv4.2ΔN-MYC consists of wild-type Kv4.2 with the first 30 amino acids deleted so that it will traffic to the cell surface more efficiently (31). *Regions inside white boxes* on low power images are shown in high power images. *Scale bars*, 10 μm. The *arrows* point to colocalized puncta.

highly concentrated in the cell body (Fig. 1*D*). In cells expressing dominant negative variants of four other kinesins found in dendrites, Kv4.2-MYC had average dendrite/cell body ratios that were significantly larger than the average for Kv4.2-MYC in GFP-DNKif17-expressing cells ($p < 0.001$), indicating that in the former cells, the channel was localized to the dendrites to a much greater extent than in the latter (Fig. 1*D*). Relatively high dendrite/cell body ratios were also obtained for Kv4.2-MYC in cells expressing introduced, full-length Kif17 (0.45 ± 0.06, $n = 33$; Fig. 1*D*). This latter control is particularly important, because it indicates that GFP-DNKif17 is probably not blocking localization of Kv4.2 by merely sequestering other proteins and preventing them from participating in localization. The mean expression levels of Kv4.2-MYC in each case were not dramatically different, which indicates that lack of transport was not due to inhibition of Kv4.2-MYC expression (Fig. 1*D*). In order to determine whether GFP-DNKif17 was blocking protein transport nonspecifically, we examined its effect on transport of CD8. We found that in cells expressing GFP-DNKif17, CD8 was localized throughout the axons and dendrites with a dendrite/cell body ratio of 0.64 ± 0.07 (Fig. 1*D*), indicating that protein transport was not blocked nonspecifically. We also confirmed that GFP-DNKif17 effectively blocked localization of introduced NR2B in slices (data not shown), and GFP-DNKif5B blocked localization of endogenous GluR2 in dissociated neuronal cultures (Fig. 1*E*), as reported previously (14, 17). Finally, to ensure that GFP-DNKif17 did not block localization of dendritically targeted proteins nonspecifically, we demonstrated that it did not block localization of endogenous GluR2 in culture (Fig. S1).

To further demonstrate that Kif17 plays an important role in localization of Kv4.2, we expressed GFP-DNKif17 in cortical neurons in dissociated culture and examined its effect on the localization pattern of the endogenous channel. We found that 48 h after expression of GFP-DNKif17, endogenous Kv4.2 was localized in the cell body and almost absent from dendrites, consistent with transport of the channel being blocked (Fig. 2*A*). CD8, which was coexpressed with GFP-DNKif17, was localized throughout the cell, indicating that protein transport was not blocked nonspecifically. As controls, we examined the localization of endogenous Kv4.2 either following expression of GFP-DNKif5B or in untransfected cells. In both cases, endogenous Kv4.2 was localized throughout the dendrites, indicating that transport was not affected (Fig. 2*B*, data not shown). We found that in cells expressing GFP-DNKif17, the dendrite/cell body ratio of endogenous Kv4.2 was 0.06 ± 0.01 (Fig. 2*C*), which is significantly lower than the ratio for either cells expressing GFP-DNKif5B (0.4 ± 0.05, $p < 0.0001$) or for untransfected cells (0.5 ± 0.2, $p < 0.0001$). From these results, we conclude that Kif17 is essential for localization to dendrites of both introduced Kv4.2-MYC and the endogenous channel and that Kv4.2 is probably transported by Kif17.

To further test the hypothesis that Kif17 transports Kv4.2 to dendrites, we examined whether the two proteins colocalize in neurons. We expressed a tagged version of the kinesin (HA-Kif17) in neurons in dissociated cultures and found that the expression pattern of HA-Kif17 overlapped with that of endogenous Kv4.2 (Fig. 3*A*). To further confirm that Kv4.2 colocalizes specifically with Kif17, we introduced a tagged

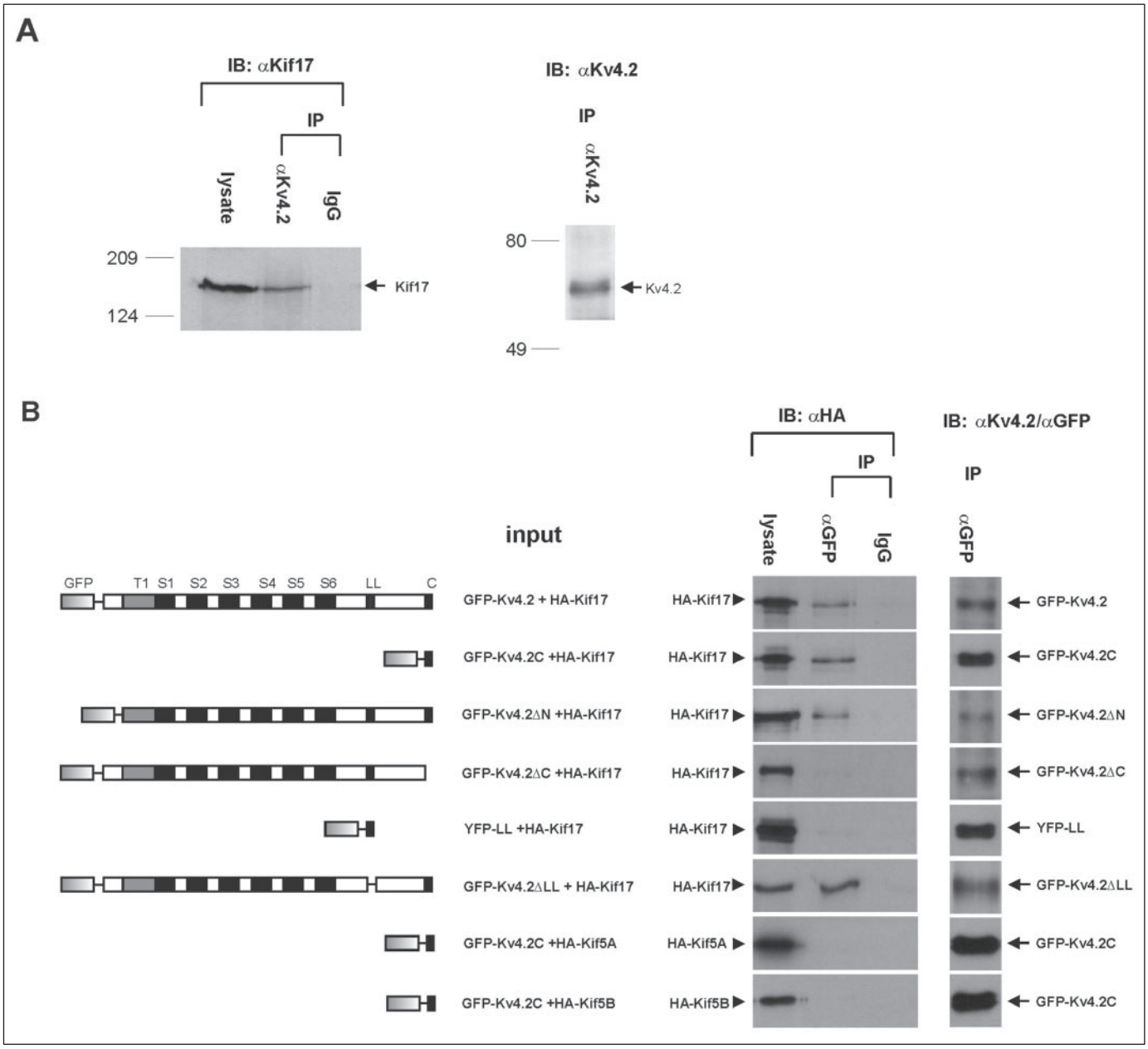

FIGURE 4. **Kv4.2 coprecipitates with Kif17.** *A*, endogenous Kv4.2 coimmunoprecipitates with Kif17 from brain lysate. The Kv4.2-Kif17 complex was immunoprecipitated (*IP*) from mouse brain homogenate using anti-Kv4.2 antibody. The complex precipitated contained both Kif17 and Kv4.2 as assessed by immunoblotting (*IB*) with anti-Kif17 and anti-Kv4.2 antibodies, respectively. In contrast, rabbit IgG did not pull down Kif17. Molecular weight markers (in kDa) are shown to the *left* of the blots. *B*, HA-Kif17 coimmunoprecipitated with full-length GFP-Kv4.2, with the 30 amino acids at the distal C terminus of Kv4.2 (GFP-Kv4.2C), with Kv4.2 lacking the 16-amino acid dileucine motif (GFP-Kv4.2ΔLL) and with Kv4.2 lacking amino acids 2–31 of the N terminus (GFP-Kv4.2ΔN). HA-Kif17 did not coprecipitate with the channel lacking the distal 30 amino acids of the C terminus (GFP-Kv4.2ΔC) or with the 16-amino acid dileucine-containing motif of Kv4.2 (YFP-LL). Neither HA-Kif5A nor HA-Kif5B coimmunoprecipitated with GFP-Kv4.2C. All pairs of proteins were first coexpressed in COS cells and then immunoprecipitated with anti-GFP antibodies from lysates and probed with anti-HA antibodies to detect kinesin isoforms. To ensure that immunoprecipitation was specific to anti-GFP, aliquots of the same lysates were also immunoprecipitated with rabbit IgG antibodies and probed with anti-HA. To ensure that, in each case, the anti-GFP antibody precipitated the GFP-tagged protein, aliquots of each lysate that had been immunoprecipitated with anti-GFP were probed either with anti-GFP (GFP-Kv4.2C and YFP-LL) or with anti-Kv4.2 (GFP-Kv4.2, GFP-Kv4.2ΔC, GFP-Kv4.2ΔN, GFP-Kv4.2ΔLL). Schematics depicting different Kv4.2 proteins expressed for immunoprecipitation are shown to the *left*.

version of the channel along with tagged versions of various kinesin isoforms into neurons in dissociated cultures. We found that introduced Kv4.2ΔN-MYC colocalized with YFP-Kif17 (Fig. 3*B*). In contrast, Kv4.2ΔN-MYC did not colocalize with either YFP-Kif5A, YFP-Kif5B, YFP-Kif21B, or YFP-KifC2 (Fig. S2).

Characterization of the Interaction between Kv4.2 and Kif17—To determine whether Kif17 associates with Kv4.2, we performed immunoprecipitation experiments using lysate from homogenized mouse brains. We found that anti-Kv4.2 antibody coimmunoprecipitated Kif17, indicating that Kv4.2 and Kif17 probably are part of a complex *in vivo* (Fig. 4*A*). To further explore the interaction between these two proteins, we expressed tagged versions of both proteins in COS-7 cells and performed coimmunoprecipitation experiments. GFP-labeled, full-length Kv4.2 and similarly labeled Kv4.2 deletion constructs were each immunoprecipitated, and the immunocomplex was probed for HA-tagged kinesins. We found that, as with the endogenous proteins, introduced HA-Kif17 coprecipitated with expressed Kv4.2 (Fig. 4*B*). Identifying the region on Kv4.2 that mediates attachment to the kinesin-containing complex could have important implications for mechanisms of dendritic targeting of the channel. In particular, we were interested in

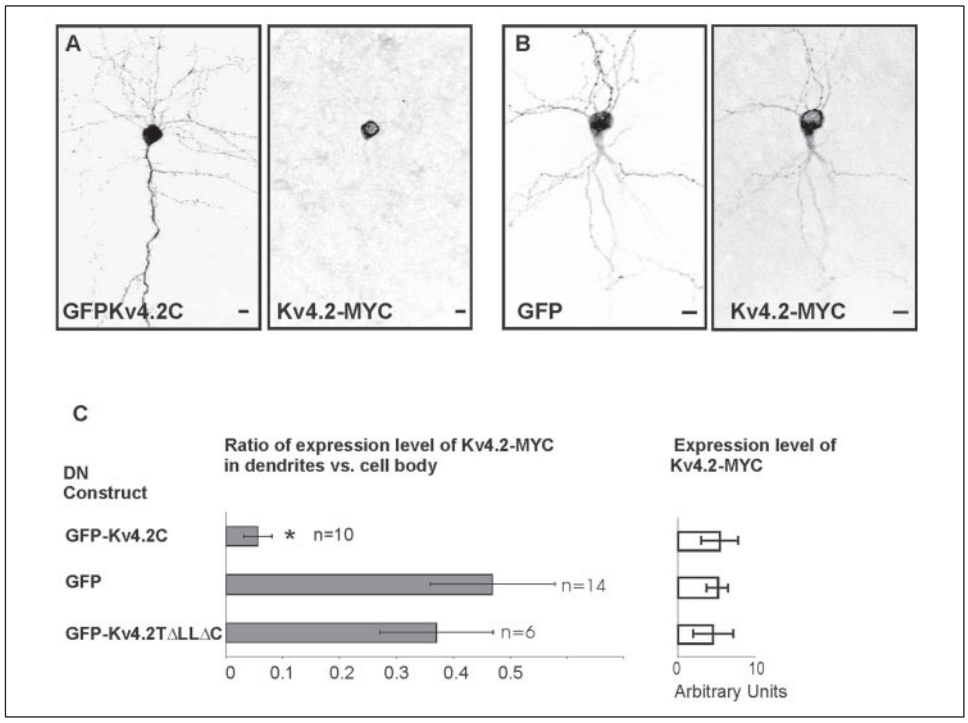

FIGURE 5. **The C terminus of Kv4.2 acts as a dominant negative to block dendritic localization of Kv4.2-MYC.** Either a protein consisting of the C-terminal 30 amino acids of Kv4.2 fused with GFP (GFP-Kv4.2C) (*A*) or GFP alone (*B*). was expressed in neurons in cortical slices, and 24 h later, expression of Kv4.2-MYC was induced in the same cells for 48 h. GFP-Kv4.2C completely blocked dendritic localization of Kv4.2-MYC, whereas GFP did not affect localization. *C*, expression of GFP-Kv4.2C prior to expression of Kv4.2-MYC caused the channel to be concentrated in the cell body, with a dendrite to cell body ratio of 0.06 ± 0.02 ($n = 10$). In contrast, in cells expressing GFP and GFP-Kv4.2TΔLLΔC (consisting of the cytoplasmic tail of Kv4.2 with the dileucine motif and the 30 amino acids at the extreme C-terminal end deleted), Kv4.2-MYC localized to the dendrites to a far greater degree, with average dendrite/cell body ratios of 0.47 ± 0.1 ($n = 14$) and 0.37 ± 0.09 ($n = 6$), respectively. The *asterisk* indicates that the dendrite/cell body ratio for Kv4.2-MYC in cells expressing GFP-Kv4.2C was significantly different from similarly calculated ratios for the channel in cells expressing GFP or GFP-Kv4.2TΔLLΔC ($p < 0.0001$). Expression levels of Kv4.2-MYC were not significantly different in cells expressing GFP *versus* cells expressing GFP-Kv4.2C or GFP-Kv4.2TΔLLΔC. Note that expression levels are measured in arbitrary units of fluorescence that are the same for each measurement. *Scale bars*, 10 μm.

knowing whether the dileucine motif of Kv4.2 mediates this attachment. A precedent for a binding scheme of this nature comes from the mannose 6-phosphate receptor, which attaches to the adaptor protein AP-1 via a tyrosine-containing targeting motif. AP-1, in turn, binds to the kinesin Kif13A (21). A second possibility is that Kv4.2 binds to the kinesin-containing complex through its extreme C terminus, in a manner similar to GluR2 and NR2B (13, 14).

To distinguish between these two possibilities, we coexpressed the 30 amino acids at the extreme C terminus of Kv4.2 (Kv4.2C, amino acids 601–630), tagged with GFP, with HA-tagged Kif17 in COS cells. Immunoprecipitation with anti-GFP antibody and immunoblotting with anti-HA confirmed that the HA-Kif17 coprecipitates with GFP-Kv4.2C, indicating that Kv4.2C is sufficient to bind, either directly or indirectly, to Kif17 (Fig. 4*B*). The extreme C-terminal region appears to also be necessary for binding of Kv4.2 to Kif17, since a recombinant protein consisting of Kv4.2 lacking these 30 amino acids, GFP-Kv4.2ΔC, does not coprecipitate with HA-Kif17 (Fig. 4*B*). In contrast, the 16-amino acid dileucine-containing motif from the C terminus of Kv4.2 (amino acids 474–489) tagged with YFP (YFP-LL) does not coprecipitate with HA-Kif17, indicating that Kif17 does not have a strong interaction with Kv4.2 through the dileucine motif. Moreover, a Kv4.2 mutant protein that lacks the dileucine motif, GFP-Kv4.2ΔLL, coimmunoprecipitates with HA-Kif17, indicating that the motif is not necessary for interaction with Kif17.

Additional experiments showed that Kv4.2 lacking the 30 amino acids at the extreme N terminus (GFP-Kv4.2ΔN) coprecipitated with HA-Kif17, indicating that this region is not necessary for interaction with the kinesin-containing complex. To test for the specificity of the interaction between Kv4.2C and Kif17, we asked whether GFP-Kv4.2C could coprecipitate with either HA-Kif5A or HA-Kif5B. Neither kinesin coprecipitated with Kv4.2C, indicating that the C terminus did not interact nonspecifically with kinesin motors (Fig. 4*B*).

The Extreme C Terminus of Kv4.2 Acts as a Dominant Negative to Block Localization—To determine whether the binding of Kif17 to the extreme C terminus of Kv4.2 is biologically relevant, we tested whether expression of GFP-Kv4.2C blocked localization of the full-length channel. If the C terminus of Kv4.2 does bind to a complex containing Kif17, it would be expected that expressing GFP-Kv4.2C at a high concentration would cause it to bind up the available endogenous Kif17 and thereby prevent the kinesin from binding to and transporting Kv4.2. Experiments in cortical slices, using the same paradigm as for the kinesin dominant negative experiments (Fig. 1*B*), showed that expressing GFP-Kv4.2C caused subsequently expressed wild-type Kv4.2-MYC to localize exclusively in the cell body (Fig. 5*A*). When Kv4.2-MYC was expressed subsequent to expression of GFP, it localized throughout the dendrites, in dramatic contrast to its localization following expression of GFP-Kv4.2C (Fig. 5*B*). To further explore whether additional regions within the cytoplasmic tail were important for localization of Kv4.2-MYC, we induced expression of the channel following expression of GFP-Kv4.2TΔLLΔC, a construct consisting of the entire C-terminal cytoplasmic tail of Kv4.2 with the dileucine motif and the 30 amino acids at the distal C terminus deleted. This construct did not obstruct localization of Kv4.2. Quantitation of the results showed that in cells expressing GFP-Kv4.2C, the dendrite/cell body ratio of Kv4.2-MYC was 0.06 ± 0.02 ($n = 10$) as compared with 0.47 ± 0.1 ($n = 14$) in cells expressing GFP alone and 0.37 ± 0.1 ($n = 6$) for cells expressing GFP-Kv4.2TΔLLΔC (Fig. 5*C*). The former value is significantly lower than the latter two ($p < 0.0001$). This result is consistent with the distal C terminus of Kv4.2 playing an important role in transport of the channel, which is, in turn, consistent with a model where Kv4.2 attaches to a complex containing Kif17 via a motif located in the extreme C-terminal region of the channel.

The Dileucine Motif Can Mediate Dendritic Targeting Independent of Kif17—From the above experiments showing that the dileucine motif of Kv4.2 does not mediate attachment to Kif17, we would predict that an exogenous protein containing this motif could be transported by a kinesin other than Kif17. If this is the case and the dileucine motif is still able to direct dendritic targeting, then we could conclude that the dileucine motif does not require interaction with a particular kinesin isoform to mediate dendritic targeting. We can test this by determining whether

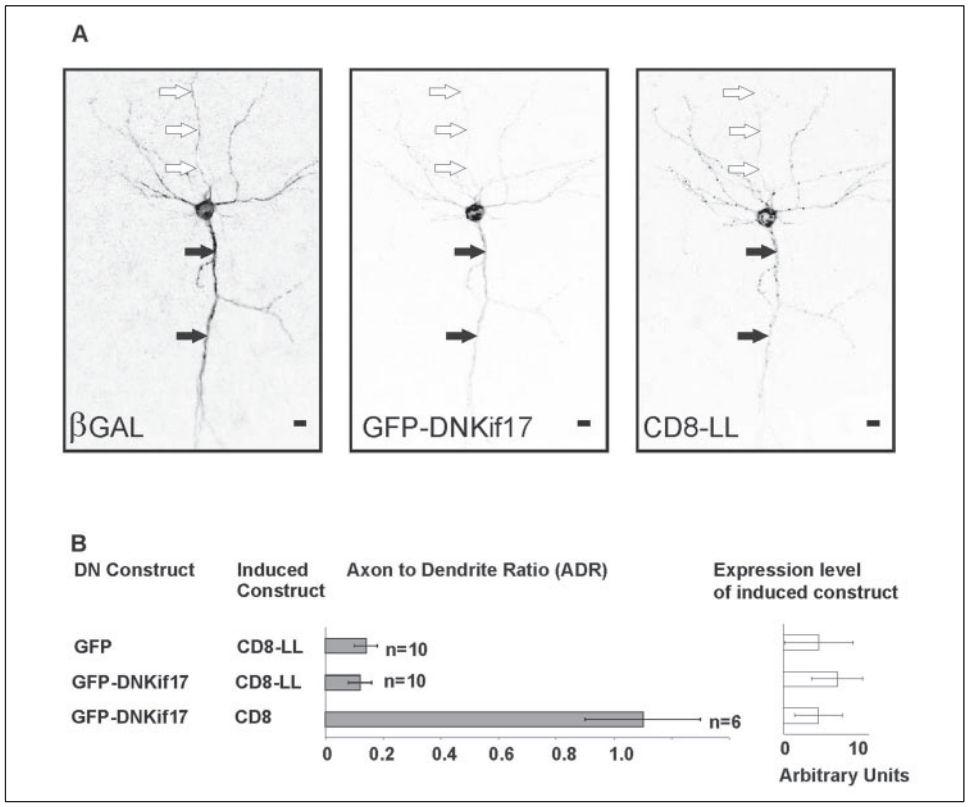

FIGURE 6. **Dendritic targeting mediated by the dileucine-containing motif does not require Kif17.** *A*, GFP-DNKif17 was initially expressed in neurons in cortical slices. After 24 h, expression of CD8-LL (CD8 with the dileucine-containing motif added to the C terminus) was induced in the same cells for 48 h. CD8-LL was targeted specifically to dendrites despite the presence of GFP-DNKif17, indicating that Kif17 was probably not necessary for transport of CD8-LL. The *unfilled arrows* point to the axon. The *filled arrows* point to dendrites. *B*, the average ADR of CD8-LL was 0.12 ± 0.04 or 0.14 ± 0.004 when expressed in the presence of either GFP-DNKif17 or GFP, respectively, indicating that GFP-DNKif17 did not block dendritic targeting. In contrast, CD8 expressed in a nonspecific manner with an average ADR of 1.1 ± 0.2. The expression level of CD8-LL was not significantly different in cells expressing GFP *versus* cells expressing GFP-DNKif17. Note that expression levels are measured in arbitrary units of fluorescence that are the same for each measurement. *DN*, dominant negative construct. *Scale bars*, 10 μm.

Kif17 transports the fusion protein of CD8 with the dileucine motif (CD8-LL), which we previously showed is localized to dendrites (10). We expressed GFP-DNKif17 in cortical pyramidal cells in slices and induced expression of CD8-LL 24 h later. We then examined the localization of CD8-LL to determine whether it could target to dendrites despite blocking the function of Kif17. Targeting of CD8-LL appeared to be unaffected by expression of GFP-DNKif17, since the receptor was clearly localized specifically to dendrites (Fig. 6*A*).

To quantify the degree of polarization of CD8-LL, we calculated the ADR, which indicates nonspecific targeting when it is close to 1 and dendritic targeting when it is less than 1. In cells that initially expressed GFP-DNKif17, CD8-LL was targeted to dendrites (ADR = 0.12 ± 0.04, $n = 10$) in a manner comparable with control cells where GFP was initially expressed (ADR = 0.14 ± 0.04, $n = 10$; Fig. 6*B*). These values are essentially indistinguishable from each other, and both are significantly different from the average value of ADR obtained when CD8 was expressed following expression of GFP-DNKif17 (ADR = 1.1 ± 0.2, $n = 6$; $p < 0.0001$). These results indicate that GFP-DNKif17 does not have an effect on dendritic targeting of CD8-LL, which suggests that CD8-LL is transported to dendrites by a motor protein other than Kif17. These data show that the dileucine motif of Kv4.2 can mediate dendritic targeting independent of the specific kinesin that is used to transport the protein.

DISCUSSION

Here we present evidence that the voltage-gated K^+ channel Kv4.2 is transported by the kinesin isoform Kif17 in cortical neurons. Kif17 or a complex containing this protein binds to Kv4.2 through the extreme C terminus of the channel and not through the dileucine-containing dendritic targeting motif. Although we showed that Kif17 both colocalized and coimmunoprecipitated with Kv4.2, the exact nature of the interaction between the two proteins was not determined. Other studies have found that kinesins interact with the C termini of the ion channels NR2B and GluR2 through proteins that contain PDZ domains (13, 14). On the basis of these results we would speculate that Kif17 probably does not bind directly to Kv4.2 but binds through a PDZ domain-containing protein that is present both in cortical neurons and in COS cells.

Our results show that Kif17 is necessary for localization of both endogenous and introduced Kv4.2 to dendrites. The most parsimonious interpretation of these results is that Kv4.2 is transported to the dendrites by Kif17 and that blocking function of this kinesin blocks transport of Kv4.2 to the dendrites. This interpretation is in keeping with the well established role of Kif17 in transporting the ion channel NR2B to the dendrites (13, 17), although there are other possible interpretations of the results of Figs. 1 and 2. For instance, blocking Kif17 function could disrupt transport or assembly of Kv4.2 in either the endoplasmic reticulum (ER) or Golgi, causing the channel to be trapped in either of those compartments. However, the facts that blocking Kif17 function with dominant negatives causes the channel to be highly localized to the cell body and that within the cell body the channel is localized in a diffuse manner argue strongly against these interpretations. If it were the case that Kv4.2 were trapped in the ER, one would expect that the channel would be distributed throughout the dendrites, since this structure is present in dendrites (22, 23). If Kv4.2 were stuck in the Golgi, it would localize in a discontinuous, sharply demarcated pattern (24) instead of a diffuse pattern (Fig. S3). However, these results do not definitively rule out a role for Kif17 in promoting exit from the ER/Golgi, and further experiments will be necessary to fully define its function in this respect. Another aspect of Kif17 function that merits further investigation is its relationship to the Kv4-interacting proteins DPPX and KChIP, which are essential for the release of the channel from the ER/Golgi. Our initial observations would suggest that Kif17 works at a point downstream of ER/Golgi exit and thus might work independently of DPPX and KChIP. However, the role of these latter proteins in trafficking events beyond

the Golgi is not known, so it is possible that DPPX and KChIP might aid Kif17 in transporting Kv4.2. It is also possible that DPPX and KChIP might interact physically with Kif17. However, KChIP binds to Kv4.2 via the N terminus and DPPX via the S1 and S2 domains, whereas Kif17 interacts with the extreme C terminus of the channel. Thus, neither KChIP nor DPPX probably plays an essential role in linking Kv4.2 and Kif17 (25, 26).

Our results indicating that the Kif17 protein complex probably attaches to Kv4.2 via the extreme C terminus and not through the dileucine-containing motif are consistent with the idea that Kif17 probably does not target to dendrites autonomously. If Kif17 could target to dendrites autonomously, then merely attaching Kv4.2 to Kif17 would be sufficient to induce dendritic targeting of the channel, which would contradict our previous finding that the dileucine motif is necessary for dendritic targeting of the channel (10). Such a prediction is also consistent with results showing that a deletion mutant of Kif17 that lacks a cargo-binding region travels to the distal regions of both dendrites and axons (27). If Kif17 does not traffic autonomously to dendrites, how might dendritic targeting of the channel be mediated? It is possible that vesicles containing Kv4.2 might be transported to both axons and dendrites and then either dock specifically to dendrites or be endocytosed from the axonal surface. However, our previous results showing that the dileucine motif is necessary and sufficient to mediate dendritic targeting of intracellular protein and that it does not mediate endocytosis would argue against this interpretation (10). Alternatively, it could be that the dileucine motif somehow modifies the function of Kif17 such that it transports Kv4.2-containing vesicles specifically to dendrites. Experiments using time lapse imaging to observe moving vesicles in living neurons will be necessary to further examine these two models.

In contrast to our results with Kv4.2, recent studies indicate that the AMPA receptor GluR2 might be targeted to dendrites through a motif that mediates attachment to a kinesin complex (14). It was shown that Kif5B binds to the PDZ domain protein GRIP, which in turn binds to GluR2 (14, 28). Moreover, when Kif5B binds to a minimal binding region of GRIP, the two proteins localize to dendrites (14), in contrast to the axonal localization of Kif5B with its cargo region deleted (27). This result indicates that GluR2 might be targeted to dendrites merely by attaching to the GRIP-Kif5B complex and suggests that the receptor would not need an additional targeting motif within its primary structure to achieve localization to dendrites. Comparison of the Kif5B results with those presented in this study suggests that different kinesin isoforms might mediate transport to specific subcompartments in neurons by distinct mechanisms.

The results shown in Fig. 6 imply that the dileucine-containing motif can mediate dendritic targeting through more than one kinesin isoform. Additional evidence suggesting that the dileucine-containing motif might work with a diversity of kinesin isoforms can be found by comparing the amino acid sequences of different members of the Shal K^+ channel family. Examination of the extreme C termini of Shal channels from different organisms indicates that this region is highly divergent despite the fact that each channel has a nearly identical dileucine-containing motif (Fig. S4). In a particularly striking example, Shal channels of the California spiny lobster, *Panulirus interruptus*, which are predominantly found in the somatodendritic compartment of pyloric neurons, could be encoded by at least 14 different splice variants producing at least five distinct C-terminal regions, yet all have conserved dileucine-containing motifs (29, 30). In the case of the Shal channel in *Drosophila melanogaster*, the dileucine-containing motif itself is at the extreme C terminus, which suggests that the channel connects to the kinesin either through the dileucine motif or through a region other than the extreme C terminus.

In conclusion, we have presented evidence that Kif17 is essential for transport of Kv4.2. Although Kif17 is also likely to play a role in dendritic targeting of the channel, defining that role will require further experiments.

Acknowledgments—We thank L. Goldstein and R. Vale for supplying kinesin constructs and Emily Liman, Michelle Arbeitman, David McKemy, and Michael Quick for critical reading of the manuscript.

REFERENCES

1. Yoshimura, Y., Yamauchi, Y., Shinkawa, T., Taoka, M., Donai, H., Takahashi, N., Isobe, T., and Yamauchi, T. (2004) *J. Neurochem.* **88,** 759–768
2. White, E. L. (1989) *Cortical Circuits*, Birkhauser, Boston
3. Tsunoda, S., Sierralta, J., Sun, Y., Bodner, R., Suzuki, E., Becker, A., Socolich, M., and Zuker, C. S. (1997) *Nature* **388,** 243–249
4. Garrido, J. J., Fernandes, F., Giraud, P., Mouret, I., Pasqualini, E., Fache, M. P., Jullien, F., and Dargent, B. (2001) *EMBO J.* **20,** 5950–5961
5. Garrido, J. J., Giraud, P., Carlier, E., Fernandes, F., Moussif, A., Fache, M. P., Debanne, D., and Dargent, B. (2003) *Science* **300,** 2091–2094
6. Cheng, C., Glover, G., Banker, G., and Amara, S. G. (2002) *J. Neurosci.* **22,** 10643–10652
7. Francesconi, A., and Duvoisin, R. M. (2002) *J. Neurosci.* **22,** 2196–2205
8. Stowell, J. N., and Craig, A. M. (1999) *Neuron* **22,** 525–536
9. Jareb, M., and Banker, G. (1998) *Neuron* **20,** 855–867
10. Rivera, J. F., Ahmad, S., Quick, M. W., Liman, E. R., and Arnold, D. B. (2003) *Nat. Neurosci.* **6,** 243–250
11. Johnston, D., Hoffman, D. A., Colbert, C. M., and Magee, J. C. (1999) *Curr. Opin. Neurobiol.* **9,** 288–292
12. Burack, M. A., Silverman, M. A., and Banker, G. (2000) *Neuron* **26,** 465–472
13. Setou, M., Nakagawa, T., Seog, D. H., and Hirokawa, N. (2000) *Science* **288,** 1796–1802
14. Setou, M., Seog, D. H., Tanaka, Y., Kanai, Y., Takei, Y., Kawagishi, M., and Hirokawa, N. (2002) *Nature* **417,** 83–87
15. Arnold, D. B., and Clapham, D. E. (1999) *Neuron* **23,** 149–157
16. Cavalli, V., Kujala, P., Klumperman, J., and Goldstein, L. S. (2005) *J. Cell Biol.* **168,** 775–787
17. Guillaud, L., Setou, M., and Hirokawa, N. (2003) *J. Neurosci.* **23,** 131–140
18. Hanlon, D. W., Yang, Z., and Goldstein, L. S. (1997) *Neuron* **18,** 439–451
19. Saito, N., Okada, Y., Noda, Y., Kinoshita, Y., Kondo, S., and Hirokawa, N. (1997) *Neuron* **18,** 425–438
20. Niclas, J., Navone, F., Hom-Booher, N., and Vale, R. D. (1994) *Neuron* **12,** 1059–1072
21. Nakagawa, T., Setou, M., Seog, D., Ogasawara, K., Dohmae, N., Takio, K., and Hirokawa, N. (2000) *Cell* **103,** 569–581
22. Horton, A. C., and Ehlers, M. D. (2003) *J. Neurosci.* **23,** 6188–6199
23. Aridor, M., Guzik, A. K., Bielli, A., and Fish, K. N. (2004) *J. Neurosci.* **24,** 3770–3776
24. Stricker, N. L., and Huganir, R. L. (2003) *Neuropharmacology* **45,** 837–848
25. Ren, X., Hayashi, Y., Yoshimura, N., and Takimoto, K. (2005) *Mol. Cell Neurosci.* **29,** 320–332
26. An, W. F., Bowlby, M. R., Betty, M., Cao, J., Ling, H. P., Mendoza, G., Hinson, J. W., Mattsson, K. I., Strassle, B. W., Trimmer, J. S., and Rhodes, K. J. (2000) *Nature* **403,** 553–556
27. Nakata, T., and Hirokawa, N. (2003) *J. Cell Biol.* **162,** 1045–1055
28. Dong, H., O'Brien, R. J., Fung, E. T., Lanahan, A. A., Worley, P. F., and Huganir, R. L. (1997) *Nature* **386,** 279–284
29. Baro, D. J., Ayali, A., French, L., Scholz, N. L., Labenia, J., Lanning, C. C., Graubard, K., and Harris-Warrick, R. M. (2000) *J. Neurosci.* **20,** 6619–6630
30. Baro, D. J., Quinones, L., Lanning, C. C., Harris-Warrick, R. M., and Ruiz, M. (2001) *Neuroscience* **106,** 419–432
31. Bahring, R., Dannenberg, J., Peters, H. C., Leicher, T., Pongs, O., and Isbrandt, D. (2001) *J. Biol. Chem.* **276,** 23888–23894